Covalentlike electronic effects in metallic liquids using an orbital-free *ab initio* method

L. E. González, D. J. González, and M. J. Stott
Departamento de Física Teórica, Universidad de Valladolid, 47011 Valladolid, Spain
(Received 12 September 2007; published 24 January 2008)

The origin of the unusual shoulder on the large-q side of the main peak of the structure factors of liquid Ga and liquid Si is studied using an orbital-free *ab initio* molecular dynamics approach. The shoulders are found to be related to pairs of atoms that come close, supporting the earlier observation for liquid Ga based on a high temperature simulation. Results for Ga at lower temperature, and for Si at several applied pressures also show the relationship of the shoulder to pairs of atoms. The electron density near typical pairs shows an accumulation of charge between the atoms which in earlier work was taken to be an indication of a covalent bond. The calculated orbital-free electronic densities show a somewhat larger charge accumulation between the atoms than the previous Kohn-Sham calculations. This result was not anticipated because the orbital-free approach had not previously been expected to describe valence bonding. However, electron density distributions for Si for atomic configurations at several pressures calculated with the orbital-free approach compare very favorably with the results of Kohn-Sham calculations for the same configurations. On the other hand, analysis of the temperature dependence of the population of pairs and of their time evolution does not support the proposal that the pairs are covalently bonded. Other factors that may also contribute to the appearance of the shoulder are discussed.

DOI: 10.1103/PhysRevB.77.014207 PACS number(s): 61.20.Ja, 61.20.Lc, 61.25.Mv, 71.15.Pd

I. INTRODUCTION

Molecular dynamics (MD) methods are a useful technique for studying the properties of liquids systems, and the past two decades have seen a large increase in the application of *ab initio* molecular dynamics (AIMD) methods based on density functional theory[1] (DFT). DFT allows calculation of the ground state electronic energy of a collection of atoms for given nuclear positions and the forces on the nuclei via the Hellmann-Feynman theorem. It enables performance of MD simulations in which the nuclear positions evolve according to classical mechanics, whereas the electrons follows adiabatically. Most AIMD methods are based on the Kohn-Sham[2] (KS) approach to DFT (KS-AIMD methods) which, at present, poses heavy computational demands that severely restrict the system size and the simulation times. These restrictions are reduced in the so-called orbital-free (OF) *ab initio* molecular dynamics (OF-AIMD) method, which, by disposing of the electronic orbitals of the KS formulation, provides a simulation method where the number of variables describing the electronic state is greatly reduced, enabling the study of larger samples (thousands of particles) for longer simulation times (tens of picosecond). However, this is at the cost of an electronic kinetic energy functional which is no longer exact and the necessity of using local pseudopotentials to describe the electron-ion interactions.

For two reasons, applications of OF methods have so far been restricted largely to simple metals and alloys.[3–10] First of all, the approximate kinetic energy functional is often constructed to be exact in the linear response limit in which the electron density is almost uniform because of a small electron-ion potential, circumstances prevailing in simple metal systems. Secondly, a good description of covalently bonded systems with directional bonding is believed to require nonlocality in the pseudopotentials which cannot be accommodated in the OF scheme. Indeed, recent attempts to apply OF methods to study the properties of crystalline Si have failed[11] for the semiconducting phases, although good results for the metallic solid phases were obtained. However, this failure may have been due to the particular kinetic energy functional and local pseudopotentials used in the study. Nevertheless, the electron density obtained from the OF method for fixed ion arrangements, e.g., the diamond structure, agreed quite well with that from full KS method calculations.

More recently,[12] OF-AIMD studies of liquid Si using 2000 particles have yielded static structural properties in good agreement with both experiment[13,14] and KS-AIMD data,[15] and simulation times were long enough to allow the study of the dynamic structure. Liquid Si has metallic properties, but it is not a typical liquid metal. Its density increases upon melting; the structure is rather open with about 6 nearest neighbors (NNs) which is, of course, larger than the 4 NNs in the diamond structure but much smaller than the 12 NNs characteristic of most simple metals. In addition, the structure factor $S(q)$ has a shoulder at the high-q side of the main peak which is absent in the $S(q)$ of simple metals. Finally, the distribution of angles between "bonds" in triplets of atoms separated by less than a characteristic bonding distance has one peak at 65° and another close to the 109° tetrahedral angle, which, again, contrasts with simple metals for which peaks appear near 65° and 116°, characteristic of an icosahedral packing. Full Kohn-Sham MD studies of liquid Si, mostly using 64 atoms, related these peculiarities to remnants of covalent bonding in liquid Si, and the analysis of the electron pseudodensity did indeed show a pileup of charge along the lines joining atoms separated by less than 2.49 Å, which cannot be explained by a mere superposition of atomic pseudodensities. This maximum separation at which "covalent-bonding-like" effects appear in the liquid is somewhat larger than the bond length in Si crystal (2.35 Å). That all these properties of liquid Si could also be seen in the

OF-AIMD results[12] seems to indicate that these covalency remnants, if this is what they are, are also present in the OF treatment. Furthermore, on application of pressure, liquid Si has been found[16] to undergo some form of structural change between 8 and 14 GPa, characterized by an increase in the nearest neighbor distance and an abrupt increase of the coordination number. These features, as well as an evolution of the bond-angle distribution function into a more simple-liquid-like behavior, were also well described by OF-AIMD simulations.[17] The electron density was not investigated in these earlier OF-AIMD studies of liquid Si,[12,17] but, here, an analysis of the electron density obtained from the OF study for a range of pressures will be described.

Liquid Ga shows similar peculiarities to Si. Its density increases upon melting, and the $S(q)$ shows a shoulder at the high-q side of the main peak.[14,18] In addition, although an increase in temperature causes a decrease in density, both the nearest neighbor distance and the distance of closest approach diminish. This is different from the behavior of simple metals and appears to indicate that the interatomic repulsion at short distances is very soft so that a higher kinetic energy enables a closer approach of two ions. Solid Ga at ambient pressure (α-Ga) is metallic, but its structure is unique, showing a mixture of covalent and metallic bondings.[19,20] The structure can be described as metallically bonded buckled planes in which each atom is covalently bonded with one in an adjacent plane. Each atom has a total of seven near neighbors, the nearest one is covalently bonded at 2.48 Å, two second neighbors at 2.69 Å, two third neighbors at 2.73 Å, and two fourth neighbors at 2.79 Å. Nevertheless, a purely metallic treatment using a pseudopotential and second order perturbation theory does yield α-Ga as the most stable structure.[21] Higher pressure phases are purely metallic, although not necessarily simple, and metastability of phases further disturbs an already complicated panorama. For instance, a tetragonally distorted face centered phase with four atoms per unit cell and initially called Ga-II (Ref. 22) was thought to be the stable phase resulting from the application of pressure to α-Ga, but this phase was later found[23] to be stable only at somewhat higher temperatures and pressures and is now termed Ga-III. The new stable Ga-II phase, obtained upon pressurization of α-Ga, was reported to be body centered cubic with 12 atoms per unit cell. However, it has recently been shown that Ga-II has instead a large unit cell containing 104 atoms, and a new Ga-V phase with 6 atoms per rhombohedral unit cell was discovered between Ga-II and Ga-III.[24]

Based on KS-AIMD simulations of liquid Ga at 1000 K using 64 particles, Gong *et al.* related the peculiarities of liquid Ga to the persistence of some covalently bonded Ga_2 dimers in the liquid.[25] The analysis of the electron density revealed a charge accumulation along lines joining two Ga atoms whenever these are close. Bonds as pronounced as those occurring in α-Ga take place for separations $\approx$2.25 Å, somewhat smaller than the bond length in the solid, and weaker bonds survive up to separations around 2.5 Å, somewhat larger than the solid case bond lengths. The picture is similar to that of liquid Si. Further analysis revealed that the number of atoms involved in these "dimers" is rather small, $\approx 5\% - 10\%$, and that these are very short lived, $\approx$0.05 ps, a lifetime about one-third the period of the stretching vibration of the dimers in α-Ga. Gong *et al.* were also able to relate the characteristic shoulder in the structure factor of liquid Ga at 1000 K to the existence of these dimers. The heavy computational demands of the Kohn-Sham approach necessitated rapid thermalization and, consequently, a high simulation temperature. However, it was argued that at lower temperatures, the concentration of the Ga_2 dimers would increase leading to a sharper shoulder in $S(q)$, and it would also seem reasonable that the dimers would live longer. KS-AIMD calculations have also been reported by Holender *et al.*, also with 64 Ga atoms and a high temperature, which, with the exception of a more free-electron-like density of states, confirmed the earlier results and gave some dynamic properties.[26]

In the following sections, results of OF-AIMD simulations of liquid Ga at 959 K using 2000 particles are presented. Analysis of the type performed by Gong *et al.* shows that the OF method reproduces all the properties previously obtained by KS-AIMD simulations. Moreover, since the computational demands are much reduced, calculations at lower temperatures have been performed and the results analyzed to check the previous predictions. A similar analysis of the results of the earlier OF-AIMD simulations of liquid Si under pressure and near melting is also presented. An investigation of the electron density in the region of examples of dimers in both liquid Ga and Si is described. The presence of bondinglike charge seen in the OF results is compared with results of full Kohn-Sham calculations for the same configurations.

II. THEORY

Full details of the OF-AIMD method are given elsewhere;[5] it suffices here to describe the main points. The approximate electron kinetic energy density functional $T_s[n]$ is the sum of the von-Weizsäcker functional and a Thomas-Fermi-like term involving an averaged density. Parameters are chosen so that $T_s[n]$ is correct in the limiting cases of a slowly or rapidly varying density and weak scattering. The resulting functional is positive definite so that non-negative energies are always obtained. The local pseudopotential is constructed from first principles to give an electron density which coincides with the all-electron density in the interstitial regions of a metallic environment.

For a given ionic configuration corresponding to one of the MD simulation steps, the electron density from the OF simulation near a selected triplet of atoms is compared with the density obtained from a Kohn-Sham calculation. To obtain this, a cube containing 64 atoms was cut around the triplet from the particular configuration of the simulation and repeated periodically. The atoms near the faces of the cube that led to unphysically short distances between the periodical images of the particles were removed and the electron density was computed using the SIESTA code.[27] The Perdew-Burke-Ernzerhof[28] generalized gradient approximation was used to treat exchange and correlation, and a Troullier-Martins pseudopotential[29] was used for the electron-ion interaction with Kleinman-Bylander projectors[30]

and nonlinear core corrections for both Ga and Si. A double-zeta basis set and 75 $\vec{k}$ points were used for each system. Atom removal near the cube faces leads inevitably to a somewhat decreased overall liquid density and also to some distortion of the ionic configuration in that region. This, of course, influences the electron density near the faces of the cube. However, the electron density around the center of the cube, where the selected triplet is located, is expected to suffer very small changes due to the removal of atoms near the boundaries since it is much more sensitive to the ionic configuration in the center of the cube.

Several structural properties are obtained from the results of the liquid simulations, including the pair correlation function $g(r)$ and the structure factor $S(q)$, which are well known; the definitions of others are described here. The radial distribution function (RDF), $G(r)=4\pi r^2 g(r)$ gives the distribution of particles about a given one taken as the origin. McGreevy *et al.*[31] introduced the partial RDF $G_i(r)$, which gives the probability of finding the ith neighbor of a particle at a distance r, so that $G(r)=\Sigma_i G_i(r)$. These functions were introduced with the objective of finding a clearer-cut criterion for a "nearest neighbor" of an atom. Several criteria are routinely used,[32] e.g., a particle that is nearer than the first minimum of $g(r)$, r_m, or one nearer than the first minimum of $G(r)$, r_M, but in some cases, especially when the liquid is peculiar, r_m and r_M differ substantially, leading to ambiguities in the calculated number of nearest neighbors or coordination number. A quantity of interest here is $P_i(r)=\int_0^r G_i(s)ds$, which gives the probability of finding an ith neighbor of a particle at a distance $\leqslant r$. The limits $P_i(0)=0$ and $P_i(\infty)=1$ are attained at finite distances $r_i^{\min}$ and $r_i^{\max}$, which define the spherical shell where the ith neighbors lay. In particular, $r_1^{\min}$ is the distance of closest approach between two atoms.

Higher order correlation functions give additional information about the local arrangement of atoms. A widely used one is the bond-angle distribution function $P(\theta)$, which gives the probability density of the angle between the lines connecting an atom and two others. Usually, P is computed for triplets of particles where the two outer atoms are closer than r_m or r_M from the central one. However, other more convenient cutoffs can be introduced, e.g., a covalent radius in the case of liquid Si.[15] If the cutoff is such that an atom has more than 2, say n, neighbors that qualify, all the $n(n-1)/2$ bond angles are included in the distribution. Also useful is a "most local" bond-angle distribution $P_{12}(\theta)$, where θ is the angle between the lines joining one atom and its first and second closest neighbors, so only one angle per triplet is included in the distribution.

In reciprocal space, the liquid structure is characterized by the structure factor $S(q)=1/N\langle F(\vec{q})F(-\vec{q})\rangle$, where there are N particles in the system and the average is taken over directions of $\vec{q}$ and over configurations, and $F(\vec{q})=\Sigma_{\ell=1}^{N}\exp\times[-i\vec{q}\vec{R}_\ell]$. Following Gong *et al.*,[25] we introduce the "bonded-atoms" structure factor $S(q,r_b)$ for those atoms with at least one neighbor within a distance r_b. It is given by $S(q,r_b)=\langle F_b(\vec{q})F_b(-\vec{q})/N_b\rangle$, where $F_b(\vec{q})=\Sigma_{\ell=1}^{N_b}\exp[-i\vec{q}\vec{R}^b{}_\ell]$ and N_b is the number of bonded atoms. Note that $S(q,r_b)$ is only meaningful for $r_b\geq r_1^{\min}$ and reduces to $S(q)$ for $r_b\geq r_1^{\max}$.

III. RESULTS

OF-AIMD simulations were performed for liquid Ga near melting and at a high temperature, and for liquid Si near melting at ambient pressure and in four pressurized states. In all cases, N ions are enclosed in a periodically repeated cubic cell of the size required to obtain the experimental ionic number densities. Given ionic positions at time t, the electronic energy functional is minimized with respect to the electron density $\rho(\vec{r})=\psi(\vec{r})^2$ written in terms of the single *effective orbital*, $\psi(\vec{r})$, which is expanded in plane waves up to an energy cutoff, E_{cut}. The energy minimization with respect to the Fourier coefficients of the expansion is performed every ionic time step by using a quenching method which results in the ground state electronic density and energy and the forces on the ions via the Hellman-Feynman theorem. The ion positions and velocities are updated by solving Newton's equations using the Verlet leapfrog algorithm with a time step Δt. After an equilibration period, t_{eq}, the liquid properties are computed during a production run lasting t_{sim}. Table I displays the parameters for the seven simulations performed.

A. Liquid Ga

The structure factor $S(q)$ obtained from the simulations is plotted in Fig. 1 together with the x-ray diffraction data of Waseda[14] and the neutron scattering data of Bellissent-Funel *et al.*[18] The calculated $S(q)$ at $T=373$ K exhibits a main peak at $q_p\approx 2.51$ Å^{-1}, the characteristic shoulder at ≈ 3.10 Å^{-1}, and the second peak at ≈ 4.87 Å^{-1}. The $T=363$ K neutron scattering results of Bellissent-Funel *et al.*[18] show a main peak at ≈ 2.53 Å^{-1} with the shoulder at ≈ 3.0 Å^{-1} and the second peak at ≈ 4.87 Å^{-1}. The calculated results for $T=373$ K overestimate the amplitude of the main peak, but the amplitude and phase of the subsequent oscillations are reproduced well. Better agreement between theory and experiment is obtained for the $S(q)$ at the higher temperature. The OF-AIMD results are similar to the KS-AIMD results for $S(q)$ obtained by Gong *et al.*[25] at $T=1000$ K and by Holender *et al.*[26] at $T=982$ K; however, the latter is noisy in the region of the first peak possibly due to the small simulated sample. Note that at the higher temperature, the peak of $S(q)$ becomes broader, covering somewhat the shoulder.

The bonded-atoms structure factor $S(q,r_b)$ for those atoms with one or more neighbors within a distance r_b is shown in Fig. 2 for several values of r_b from $r_1^{\min}$ to $r_1^{\max}$. For $T=959$ K, the main peak of $S(q,r_b)$ for $r_b\leq 2.38$ Å is at the position of the shoulder of the full $S(q)$, but around $r_b=2.38$ Å, a second peak emerges at a smaller q value, which grows as r_b increases to become the main peak of $S(q)$. This is the same behavior found in the KS-AIMD simulations of Ga at 1000 K by Gong *et al.*[25] It suggests that the shoulder in $S(q)$ is directly related to the existence of atoms separated by distances less than ≈ 2.38 Å. Moreover, Gong *et al.* noted that for these separations, the electron density along the line

TABLE I. Simulation parameters and thermodynamic states studied. The temperature is given in K, the density in atoms/Å^3, the energy in Ry, the time step in units of 10^{-3} ps, and the equilibration and simulation times in ps.

System	T	ρ_i	N	E_{cut}	Δt	t_{eq}	t_{sim}
Ga	373	0.0512[a]	2000	15.50	5.0	15	80
Ga	959	0.0490[a]	2000	15.50	5.0	15	80
Si[b]	1750	0.0555[c]	2000	12.75	3.5	10	50
Si[d]	1503	0.0580[e]	2000	15.75	3.5	10	65
Si[d]	1253	0.0600[f]	2000	15.75	3.5	10	65
Si[d]	1093	0.0670[g]	2000	15.75	3.5	10	65
Si[d]	1270	0.0710[h]	2000	15.75	3.5	10	65

[a]Reference 33.
[b]Reference 12.
[c]Reference 14.
[d]Reference 17.
[e]Reference 16. Pressure: 4 GPa.
[f]Reference 16. Pressure: 8 GPa.
[g]Reference 16. Pressure: 14 GPa.
[h]Reference 16. Pressure: 23 GPa.

joining the atoms displays a charge accumulation akin to the bonding charge of the Ga_2 dimers found in solid α-Ga. They went on to suggest that the shoulder in $S(q)$ is related to the survival of these "molecules" after melting, which, although short lived, appear in appreciable concentration.[25] The variation of $S(q,r_b)$ with r_b is the same at the lower temperature, $T=373$ K. The shoulder of $S(q)$ is at the position of the main peak of $S(q,r_b)$ for small r_b, but a second peak at lower q emerges around $r_b=2.38$ Å and develops into the main peak of $S(q)$.

The pair distribution functions $g(r)$ for the two temperatures are shown in Fig. 3 along with the experimental data of Bellissent-Funel *et al.* for 326 and 959 K.[18] The position of the main peak is usually identified with the average nearest neighbor distance, which, in the present OF-AIMD calculation, is ≈2.81 Å for $T=373$ K and reduces to ≈2.73 Å for $T=959$ K. This reduction is in good agreement with the experimental results, 2.77 and 2.71 Å, respectively, and reflects the softness of the interionic repulsion for short distances. An estimate of the number of nearest neighbors, also known as the coordination number N_C, is obtained by integrating the RDF up to the position of the first minimum of the RDF at r_M.[31,32] These positions are ≈3.81 and 3.45 Å for $T=373$ and 959 K leading to $N_C \approx 11.8$ and 8.5 atoms, respectively. A similar calculation using the experimental $g(r)$ of Bellissent-Funel *et al.*[18] gives $N_C \approx 10.5$ and 8.7 atoms for $T=326$ and 959 K, respectively. The earlier KS-AIMD results at $T=1000$ and 982 K gave $N_C \approx 8.9$ and 9.1, respectively.[25,26]

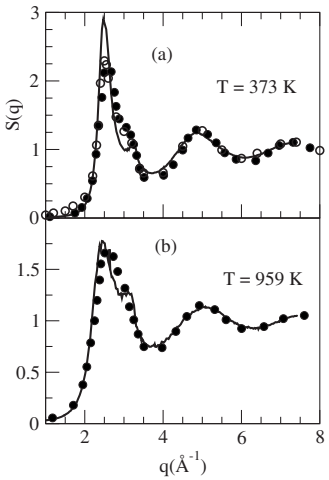

FIG. 1. Static structure factors of liquid Ga. Continuous line: OF-AIMD simulations at $T=373$ and 959 K. Full circles: experimental neutron scattering data (Ref. 18) at $T=363$ and 959 K. Open circles: experimental x-ray diffraction data (Ref. 14) at $T=323$ K.

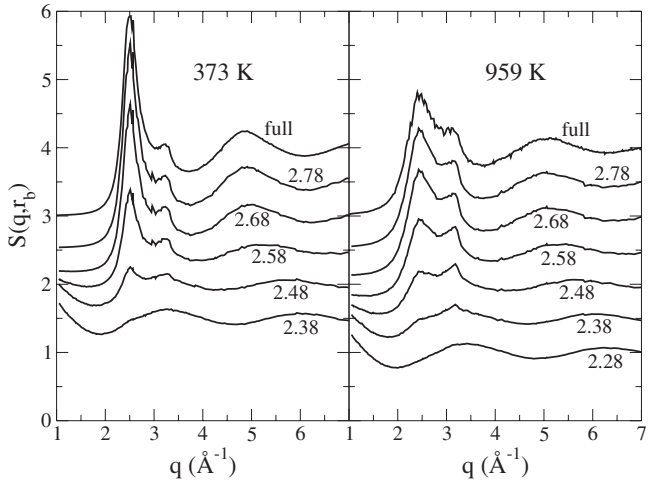

FIG. 2. Bonded-atoms structure factors of liquid Ga for different cutoff radii r_b. At 373 K, no data for $r_b=2.28$ Å are shown since that value is too close to r_1^{min} at that temperature to give meaningful results.

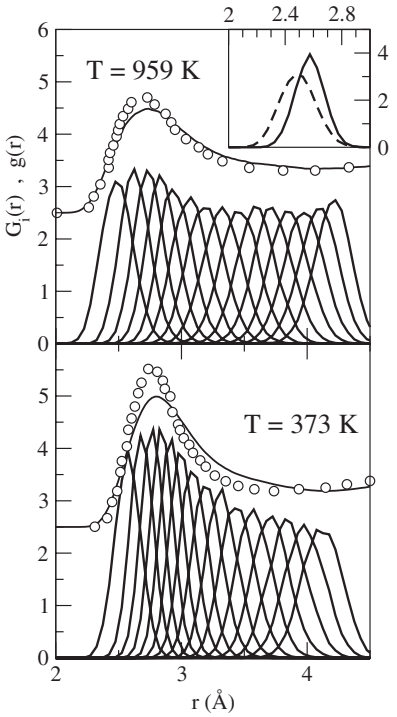

FIG. 3. Partial radial distribution functions $G_i(r)$, $i=1,\ldots,15$, of liquid Ga at $T=373$ and 959 K. The $g(r)$ are also shown (displaced 2.5 units upward) along with the experimental neutron scattering data (Ref. 18) at $T=326$ and 959 K (circles). The inset shows $G_1(r)$ for 373 K (solid line) and 959 K (dashed line).

The $G_i(r)$ at the two temperatures considered are shown in Fig. 3, along with the pair correlation function $g(r)$, which follows the heights of the $G_i(r)$. The inset highlights the variation with temperature of $G_1(r)$ for the first neighbor. There is a noticeable displacement of $G_1(r)$ to smaller distances at the higher temperature, with $r_1^{\min}$ moving from 2.25 at 373 K to 2.13 Å at 959 K, while $r_1^{\max} \approx 2.90$ for both temperatures.

Given $G_1(r)$, it is easy to compute the average concentration $x(R)$ of atoms whose first neighbor is closer than a distance R from $x(R)=P_1(R)=\int_0^R G_1(r)dr$ or its inverse $R(x)$. In the KS-AIMD simulations of liquid Ga at 1000 K of Gong *et al.*,[25] it was found that for typical covalent bonding distances, say, $R=2.35$ Å, the $x(R)\approx 5\%-10\%$. For our simulations at 959 K, $x(2.28)=0.04$ and $x(2.38)=0.18$, in good agreement with the KS study. These covalently bonded atoms were interpreted as short-lived molecules whose effects were found to be important in explaining the origin of the shoulder in the structure factor. It was also predicted that the concentration of molecules should increase at lower temperatures leading to a sharper shoulder. However, inspection of $G_1(r)$ in the inset of Fig. 3 shows that at $T=373$ K, the distance of closest approach is larger, so $x(R)$ will be smaller than at the higher temperature; in fact, at $T=373$ K, $x(2.28)\approx 0$ and $x(2.38)=0.03$. Contrary to the prediction of Gong *et al.*,[25] the OF simulations have fewer of these close neighbors at the lower temperature, which puts a first question mark against their interpretation that these atoms form molecules, even though the shoulder in the structure factor is indeed sharper at the lower T. Of course, it may be that the relevant parameter in defining these molecules is not the separation of the atoms but the accumulation of electronic density between them, a point to which we will come to later.

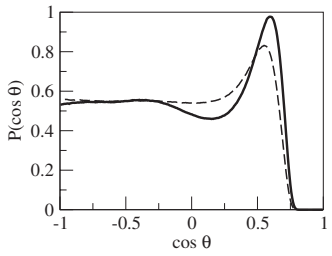

FIG. 4. Bond-angle distribution function $P(\cos(\theta))$ for liquid Ga at $T=373$ K (continuous line) and $T=959$ K (dashed line). The cutoff distance is the first minimum of their respective radial distribution functions.

The OF-AIMD results for $P(\cos(\theta))$ with neighbors taken up to r_M are plotted in Fig. 4. The distributions at the two temperatures considered are similar. For $T=373$ K, there are two maxima at $\theta\approx 53°$ and 110° and a minimum around $\theta \approx 78°$, while for the higher temperature $T=959$ K, there is only one clear maximum at $\theta\approx 56.5°$ and a very flat distribution at larger angles. The most local bond-angle distribution function $P_{12}(\cos(\theta))$ is also shown in Fig. 5; the peaks at angles near 60° are depleted with, again, rather flat distributions for larger angles. The calculation of P_{12} can be restricted to those triplets in which the distance to the first neighbor, r_1, is smaller than a given cutoff. The symbols in Fig. 5 show these functions for triplets with $r_1<2.38$ Å. Also shown as vertical lines is the bond-angle distribution for solid α-Ga, considering all the seven nearest neighbors, while the arrows denote the angles between the first and second neighbors of an atom in the solid ($\approx$106° and 140°).

Even though the full bond-angle distribution of α-Ga spans a large number of angles, the distribution of angles in liquid Ga seems to have little relation to that of the solid, especially for the most local distribution for which no features are present at the angles for the solid. Nevertheless, there are indeed triplets of particles at these angles, and in

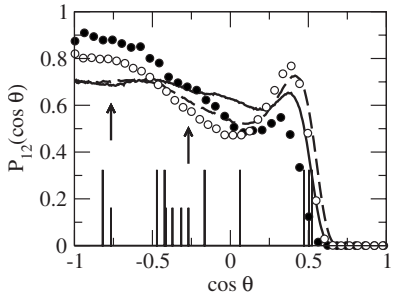

FIG. 5. Most local bond-angle distribution functions $P_{12}(\cos(\theta))$ for liquid Ga at 373 K (continuous line) and 959 K (dashed line). Symbols denote the same function when triplets are restricted to have a first neighbor distance smaller than 2.38 Å. Full circles correspond to 373 K and open circles to 959 K. Vertical lines denote the angles between an atom and any two of its seven nearest neighbors in α-Ga, while the arrows indicate the most local ones.

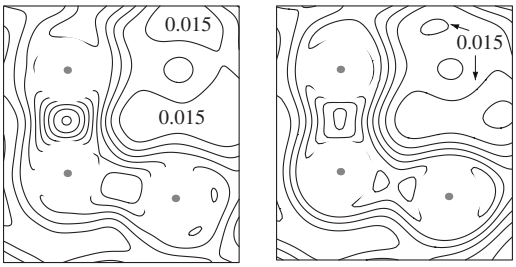

FIG. 6. Electron density for a selected triplet of Ga atoms at 373 K. Left panel: OF density. Right panel: KS density. The contour lines are plotted for values of the density equal to 0.010 electrons/a.u.[3] (the minimum inside the peanut-shaped line in the right part of the KS data) and increments of 0.005 electrons/a.u..[3] Contour lines within the core radius (≈0.75 Å)of each atom have been deleted as the pseudodensity within the core has no physical meaning.

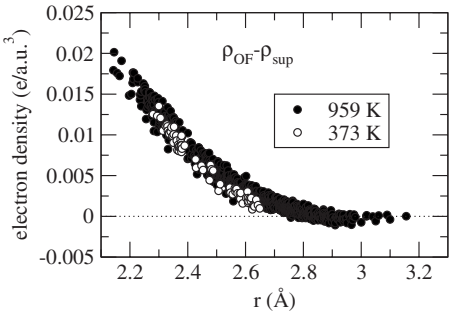

FIG. 7. Difference between the OF density and the superposition obtained from the linearly screened pseudopotential at its maximum value between two atoms separated by a distance r. The atoms considered in the plot are those with a neighbor within 2.38 Å and their first, second, and third neighbors.

the following, we discuss the electron density in a plane through one such triplet and compare it with that of the solid. The distances between the central and outer atoms are 2.35 and 2.55 Å and the bond angle is 103°. The distances for the corresponding triplet in α-Ga are 2.48 and 2.69 Å and the angle is 106°, so the distances in the liquid are about 5% smaller than in the solid. The electron density has been compared with that obtained from a full Kohn-Sham calculation using the procedure described in Sec. II. The density contours corresponding to the OF and KS calculations are shown in Fig. 6.

The similarity is striking between the densities in the liquid and in solid α-Ga in the regions between the atoms (see, for instance, Fig. 7 in Ref. 20). We also see similar electronic densities when comparing the OF density for the ionic configuration concerned, obtained from our OF simulations, and the KS density obtained for a typical ionic configuration of the KS simulations of Gong *et al.* for the liquid [see Fig. 3(a) in Ref. 25. However, more relevant to this paper is the overall agreement between the densities obtained by the OF method and the KS calculation for the same ionic configuration. Of course, there are differences, for instance, in the lower-right corner or to the right where the KS density shows a somewhat smaller minimum than the OF one, but, in general, the comparison between the densities is very favorable. It is also noted that the OF method tends to overestimate the electron density between the atoms, suggesting even stronger bonds than those obtained with the full KS method.

A good approximation to the electron density for a simple metal is the superposition of pseudoatom densities obtained from linear response screening of the pseudopotential. This superposed density also increases between the atoms as they come close enough. An analysis of the OF density between pairs of atoms including first, second, and third neighbors shows that the charge accumulation depends strongly on the distance between the atoms; the shorter the distance, the stronger the effect. Furthermore, the accumulation clearly exceeds that of the superposed densities for small separations and approaches the superposed density as the atoms separate, as shown in Fig. 7 for both temperatures. This correlation between distance and bonding charge justifies using the distance between two atoms in order to identify them as bonded.

Because of the large number of atoms in our simulations (2000), triplets, such as those shown in Fig. 6, that resemble the local arrangement of an atom in the solid can be found, but these are rare. Usually, the second neighbors are rather far from the central atom, leading only to minor increments in the density over the metallic superposition, e.g., even in the triplet shown, the second distance is 2.55 Å, rather larger than the cutoff distance of 2.35 Å. An analysis of several configurations shows that in the case of liquid Ga at both of the temperatures considered, it is almost entirely pairs of atoms that display covalentlike bond density.

The temporal behavior of these pairs of atoms is also of interest because they would be expected to be long lived if bound together and execute oscillations while close. The distribution of lifetimes of pairs, $p(t)$, during which the distance between the two atoms involved is less than 2.38 Å, is shown in Fig. 8. The most probable and the average lifetimes are very similar at both temperatures and are very short. At 959 K, the lifetime is ≈0.045 ps, very similar to the Kohn-Sham results of Gong *et al.*,[25] but at the lower temperature, the lifetime is an even shorter 0.035 ps. This shorter lifetime of the pairs at the lower temperature places a second question mark against the interpretation of them as molecules. Furthermore, analysis of the distance between the atoms as a function of time while they are closer than 2.38 Å shows that for an overwhelmingly large fraction of pairs at both tem-

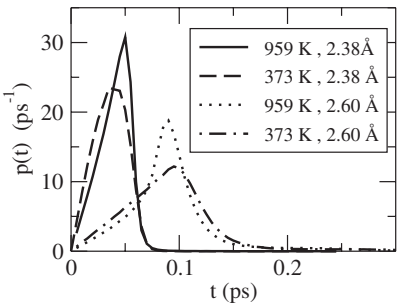

FIG. 8. Distribution function of lifetimes of pairs of atoms within a distance of 2.38 or 2.60 Å at both temperatures studied.

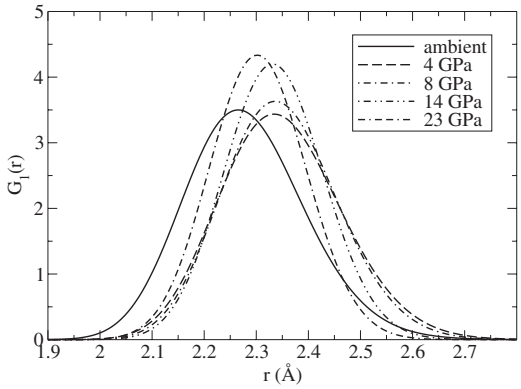

FIG. 9. Partial RDF for the first neighbor in liquid Si for several pressures.

peratures, the atoms approach, slow, stop, reverse, and depart, with no sign of vibration. As the temperature is lowered, not only are these pairs less abundant but they are also shorter lived and do not undergo vibration, features that are counterintuitive to the behavior of molecules as a function of temperature. Of course, there is uncertainty as to the definition of a pair with covalentlike character. Figure 7 shows that pairs separated by less than ≈2.6 Å already exhibit some charge accumulation and, therefore, some degree of covalentlike character could be assigned to them. Distributions of lifetimes for these pairs are also shown in Fig. 8. As expected, these pairs live longer, ≈0.09 ps, and slightly longer at the lower temperature than the higher. Even so, even the lifetime of these marginal pairs is still very short.

B. Liquid Si

A study of the static and dynamic structure of liquid Si at the thermodynamic states shown in Table I based on OF-AIMD simulations was reported in Refs. 12 and 17. Here, we discuss the partial RDFs, the most local bond-angle distribution function, the bonded-atoms structure factor, and the temporal properties of pairs of bonded atoms obtained from those same simulations. In addition, the electron densities in a plane containing a triplet of atoms obtained from the orbital-free and Kohn-Sham calculations are presented and compared, and the relation between interatomic distance and bonding density is shown.

The partial radial distribution for the first neighbor in liquid Si, $G_1(r)$, is shown in Fig. 9. The distance of closest approach, $r_1^{\min}$, is ≈1.9 Å at ambient pressure and has the larger common value of 2.0 for Si at the higher pressures, which suggests a harder effective repulsion between the atoms when pressure is applied. The width of the first neighbor shell is seen to change with pressure, leading to narrower and higher $G_1(r)$ functions, showing a clear change between 8 and 14 GPa, further supporting the idea of a structural transition between these two pressures.

Figure 10 gives examples for two pressures of the bonded-atoms structure factor $S(q,r_b)$, which follow the same pattern as liquid Ga. For small values of r_b, there is a peak at the position of the shoulder of $S(q)$, while at larger r_b

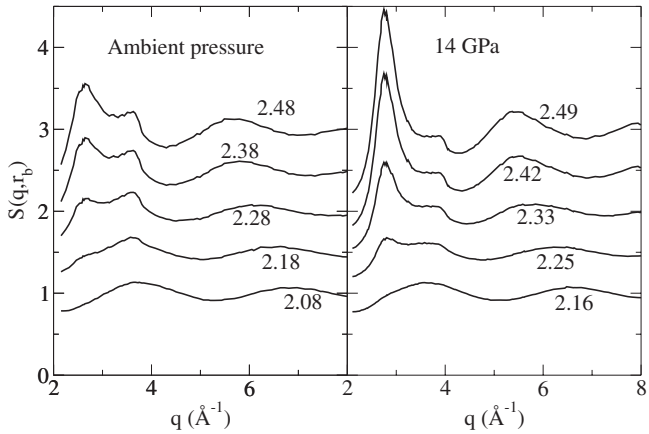

FIG. 10. Bonded-atoms structure factor of liquid Si at ambient pressure and 14 GPa. Labels with the curves denote the values of r_b in Å.

values, a feature emerges that develops into the main peak of $S(q)$ as r_b is increased. The cutoff distance R_c for the atoms to be considered as bonded has been taken as the value of r_b for which the feature at the position of the main peak of $S(q)$ starts developing and for which the shape of the $S(q,R_c)$ is similar for all the pressures studied (and also similar to that of liquid Ga). This criterion does not give a clear-cut value for R_c but is sufficient for qualitative considerations. The values of R_c in Å selected for the different pressures are 2.20, 2.25, 2.22, 2.19, and 2.16 at 0, 4, 8, 14, and 23 GPa, respectively. The corresponding $S(q,R_c)$ are shown in Fig. 11. The concentrations of bonded atoms, obtained from integration of $G_1(r)$ up to R_c, are, respectively, 0.26, 0.19, 0.11, 0.06, and 0.05. This suggests that at ambient pressure near melting, many more atoms are covalently bonded in liquid Si than in liquid Ga and that applied pressure reduces this number significantly, taking on values similar to those of liquid Ga near melting for pressures around 14 GPa.

The bond-angle distribution function obtained from the earlier OF-AIMD simulations[12,17] was similar to the KS-AIMD results at ambient pressure,[15] with peaks near 60° and

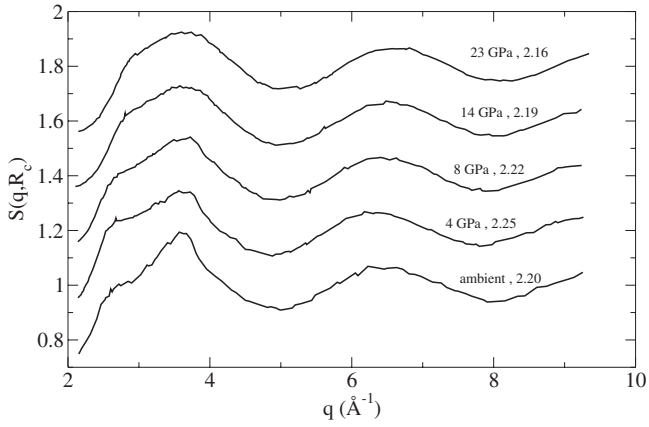

FIG. 11. Bonded-atoms structure factor of liquid Si at several pressures for the selected values of R_c (in Å) shown with each curve.

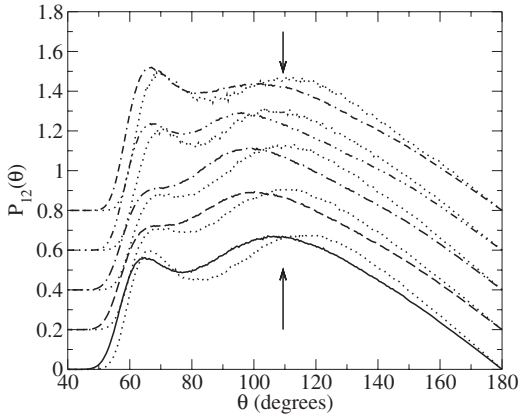

FIG. 12. Most local bond-angle distribution function in liquid Si at different pressures. The meaning of the line styles is as in Fig. 9. The dotted line denotes the same function obtained from triplets where the first neighbor of the central particle is within a distance R_c. The arrows are located at the tetrahedral angle.

90°. However, upon pressurization, a gradual change in $P(\cos\theta)$ occurred from shapes similar to that of liquid Si at ambient pressure to those resembling a good metal with peaks near 60° and 120°. More details of these changes are displayed in the most local distribution $P_{12}(\theta)$ for the first and second neighbors shown in Fig. 12. At ambient pressure, the most probable angle is rather close to the tetrahedral angle, with a subsidiary peak near 65°. Upon pressurization to 8 GPa, the main peak moves to somewhat smaller values, while the peak near 65° becomes less defined. For pressures larger than 14 GPa, the 65° peak is strengthened, becoming the dominant one, while the second peak moves to larger angles. The dotted lines in Fig. 12 show that the changes in P_{12} are much smaller if the first neighbor is within R_c. The maximum near the tetrahedral angle persists for all the pressures suggesting that even at high pressures, there are remnants of covalency, although they are few. This trend with applied pressure toward a more metallic behavior is consistent with the increase in the coordination number noted in the earlier report of the orbital-free simulations.[17] The CN grew from 6.6 at low pressure to 11.0 at 23 GPa, a value which is characteristic of a liquid metal, and with an abrupt change between 8 and 14 GPa.

The electron density in a plane containing a triplet of atoms again provides a means to visualize the degree of covalency and the OF results can be compared with those obtained from KS calculations for all the pressures considered in Fig. 13. The distances between the atoms in the vertical pair (specifically 2.14, 2.08, 2.21, 2.14, and 2.15 Å) are smaller than the R_c for the corresponding pressure, and the distances for the other pair are, respectively, 2.25, 2.21, 2.23, 2.25, and 2.24 Å, which are close to the R_c values. The corresponding angles are 111°, 106°, 107°, 99°, and 101°, respectively. The overall agreement between the OF and KS densities is again impressive in the regions shown, and in the interatom regions, the OF density shows an accumulation that is even larger than in the KS case. Also, the accumulation is larger for the shorter of the two bonds, indicating a correlation between interatomic distance and charge accumulation.

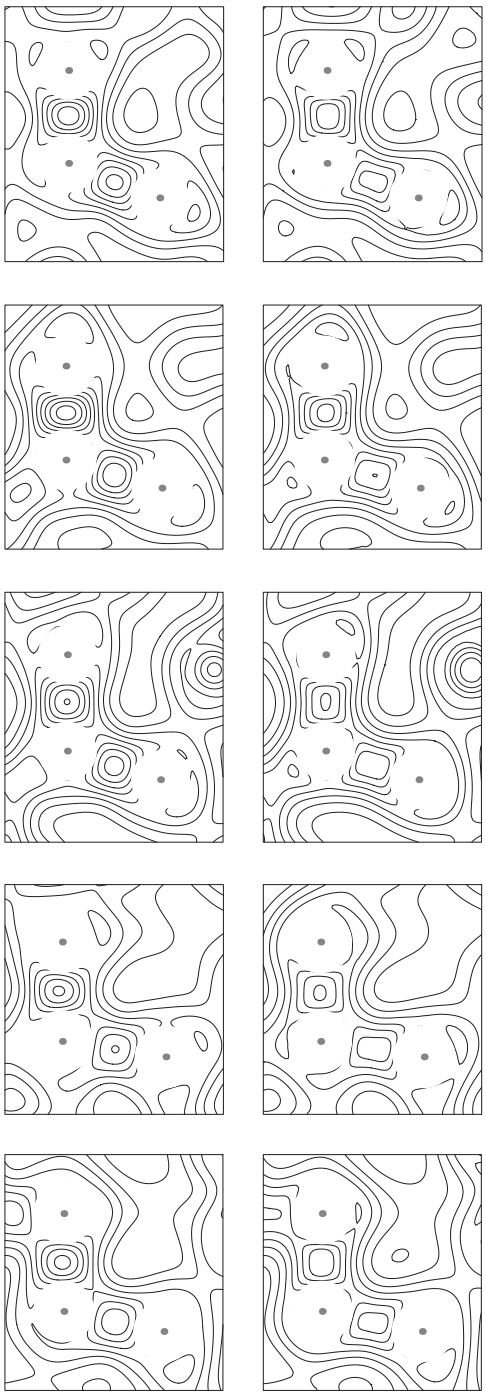

FIG. 13. Electron density around selected triplets for liquid Si. Left panels correspond to OF results and right panels are KS densities. From top to bottom, the pressures are ambient pressure and 4, 8, 14, and 23 GPa. Contour lines start at 0.02 electrons/a.u.^{3} with increments of 0.01 electrons/a.u.^{3}, and the lines within the core radius ≈0.675 Å have been omitted.

This correlation can be tested, as it was for Ga, by plotting the maximum difference between the self-consistent density and the superposition of the pseudoatom density appropriate for a metallic system along the line joining the two atoms as a function of their separation. The results for all the pressures are displayed in Fig. 14 and support the inverse length-strength correlation. Moreover, it is seen that when

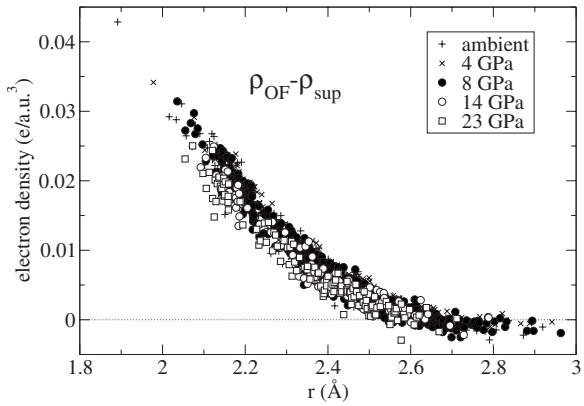

FIG. 14. Difference between the OF density and the superposition obtained from the linearly screened pseudopotential at its maximum value between two atoms separated by a distance r. The atoms considered in the plot are those with a neighbor within a distance R_c and their first, second, and third neighbors.

the atoms are further apart than about 2.6 Å, the metallic superposition becomes an excellent approximation.

The distributions of lifetimes of the Si pairs with separations smaller than R_c for the different pressures are shown in Fig. 15. As for Ga, the most probable lifetimes are all very short: about 0.02 ps up to 8 GPa, half this value at 14 GPa, and slightly longer at 23 GPa, and it appears that the structural rearrangement between 8 and 14 GPa is accompanied by some change in the dynamical behavior. These small lifetimes and also the analysis of the time variation of the distance between atoms of the pairs suggest, as for Ga, dynamical characteristics of collisions rather than binding. The distributions for pairs separated by less than the larger distance of 2.50 Å, independent of pressure, was also calculated but are not shown to avoid congestion. These distributions are qualitatively similar to those shown but are shifted to larger time. The change in the dynamics between 8 and 14 GPa was still evident.

IV. DISCUSSION

The OF results for liquid Ga show the same sort of charge accumulation between two atoms when they are close

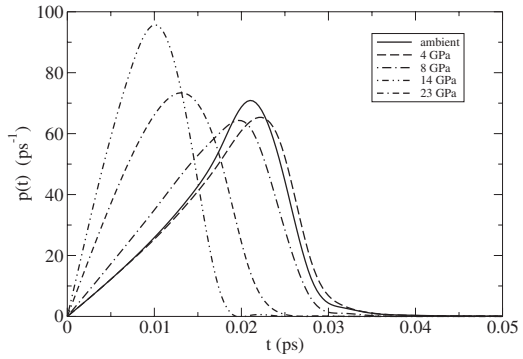

FIG. 15. Distribution function of lifetimes of pairs of Si atoms within a distance of R_c for the pressures indicated.

enough that was first reported by Gong *et al.*[25] in their KS simulation and which resembles the density in covalent bonds. It is surprising that the OF method reproduces bondlike features which are usually associated with molecular orbitals, when, as the name suggests, the method is free of orbitals. Moreover, the OF results show a larger accumulation than the results of our KS calculations for the same atomic configuration. The OF simulations of liquid Si for a number of applied pressures show similar bondlike charge accumulation which is larger than that obtained with the KS method.

Gong *et al.* also proposed that the shoulder in the structure factor of liquid Ga at about 1000 K is related to the presence of pairs of atoms separated by less than some cutoff radius, e.g., 2.38 Å. The OF results support this proposal and also find the same relation at a lower temperature close to the melting point and for liquid Si at a number of pressures. However, Gong *et al.* went on to interpret these pairs of atoms in the case of liquid Ga as covalently bonded molecules that have survived melting from the solid α-Ga structure but this interpretation is not supported by the OF results. The results show fewer pairs related to the shoulder in the lower temperature simulation, which is counter to expectation of a bound molecular unit. Also, the time evolution of pairs is more like a binary collision than a transient binding.

The relation between the atom pairs and the shoulder in the structure factors of liquid Ga and liquid Si nevertheless still remains, and the question then becomes the origin of the pairs and the charge accumulation between the atoms. In the case of liquid Ga, the interatomic repulsion is known to be very soft, which will allow atoms to become close and electronic charge to accumulate between them. This effect would explain the greater concentration of pairs at the higher temperature because of the higher atomic kinetic energy allowing atoms to come closer. Another factor that might contribute both in Ga and Si is their metallic nature. The position of the shoulder in $S(q)$ for both systems is near $q=2k_F$, which is an important wave vector for the homogeneous electron gas, which itself is the basis of many models of simple metal systems. Furthermore, a purely metallic treatment of liquid Ga using pseudopotential treated to second order in perturbation theory, along with classical simulations[34] or with liquid state theories,[35] does yield an $S(q)$ with a shoulder. Similar structure factors are also obtained for Si through the use of the same methods (second order perturbation theory and liquid state theories) with pseudopotentials constructed within the same spirit as those used in this paper.[36] Screened dispersion interactions between Ga ions also appear to have some influence on the shoulder.[37] Finally, induced polarization effects that do not vanish because of the lack of symmetry in the instantaneous ionic configurations have been found to increase the height of the shoulder and diminish the main peak.[35] In summary, the existence of pairs of atoms which show charge accumulation between them appears to be an important factor in the appearance of the shoulder of $S(q)$, but there may well be others and the picture is not yet complete.

In liquid Ga, analysis of the connection of atoms to one another showed that it is only disconnected pairs that exhibit charge accumulation resembling covalent bonds between the

atoms. A similar analysis in the case of liquid Si gave an average number of connections per atom which depended on the pressure. At ambient and low pressures, there was a mixture of pairs and open triplets of atoms with the fraction of triplets diminishing with pressure becoming very small even by 8 GPa, so that for this and higher pressures, disconnected pairs dominated. However, the number of atoms involved is 25% in the case of liquid Si, much larger than the 5% in Ga. The open triplets detected in liquid Si have a bond angle close to 109° but they exist only for a very short time, and it is premature to interpret these as remnants of the tetrahedrally bonded solid that persist into the liquid.

V. CONCLUSIONS

Orbital-free *ab initio* simulations have been performed for liquid Ga at two temperatures and used to investigate the origin of the unusual shoulder on the large-q side of the structure factor. The results suggest that the appearance of the shoulder is related to a population of pairs of atoms which are closer than a cutoff distance of about 2.38 Å, supporting the earlier proposal of Gong *et al.* based on Kohn-Sham simulations at 1000 K.[19] However, the analysis of the OF results also shows that the concentration of pairs at the higher temperature, $T=959$ K, is larger than at 373 K, which is contrary to the prediction of Gong *et al.* Similarly, the analysis of OF simulations of liquid Si at several pressures suggests that the shoulders which are also seen in the structure factors are related to atom pairs which are closer than distances that depend on the pressure but lie between 2.0 and 2.5 Å.

The electron density between the atoms of the pairs that are related to the shoulder shows an accumulation that resembles a covalent bonding charge, and this was taken by Gong *et al.* as a signature of a molecular unit. The OF approach is often thought to be limited to systems where variations in electron density are small such as simple metals and alloys, but the OF simulations also show a covalentlike accumulation which is, unexpectedly, larger than that obtained with KS calculations. Nevertheless, the effect of temperature on the population of pairs in liquid Ga and the time evolution of pairs do not support the interpretation of pairs as molecular units that have survived melting. The pairs and triplets related to the shoulders in the liquid Si structure factors are also very short lived and their behavior is collisionlike and does not resemble binding.

The portrayal by the OF method of the charge accumulations is surprising. It was not anticipated that the approach would give such a reasonable description of the large charge accumulations, even though the liquid Ga and Si systems are metallic. The success of the method reported here might signal an extension of its range of validity. However, there remain serious limitations which should be the subjects of further study. The key element of the OF method is an explicit functional of the density for the electron kinetic energy. This eliminates the need for the set of Kohn-Sham orbitals but at the cost of an approximate kinetic energy. However, the functional adopted here involves a uniform gas reference system with a mean density appropriate for the system to be investigated, and to some extent, the functional is tailor made for the particular system and may have limited transferability. The second limitation which emerges as a consequence of the elimination of the orbitals is the need for a local pseudopotential. The nonlocal, first principles pseudopotentials usually employed in *ab initio* Kohn-Sham simulations are obtained from an all-electron free atom calculation and the norm conservation guarantees transferability of the potential to other situations. The local pseudopotentials used in these OF simulations are fitted to the atom in an electronic environment similar to that in the liquid metal systems under study. Their transfer to the the particular system is likely to be very good, but transfer to the same atoms in a different environment will be less good. The method to construct the pseudopotentials, making explicit use of the OF functional in its unscreening, attempts to achieve some cancellation of the errors inevitably present in the functional. The success of the method here and earlier suggests that this is in fact the case.

The development of a kinetic energy functional that does not require a uniform gas reference system or is insensitive to the choice of system is worthy of study. A uniform gas is also involved in the generation of the pseudopotential and it may be possible to select from the set of potentials the one which is insensitive to the mean density of the gas.

ACKNOWLEDGMENTS

The financial support of the Ministerio de Educación y Ciencia of Spain (MAT2005-03415), Junta de Castilla y Leon (VA068A06), and the EU Feder Program is acknowledged. M.J.S. acknowledges the suport of the NSERC of Canada.

[1] P. Hohenberg and W. Kohn, Phys. Rev. **136**, B864 (1964).
[2] W. Kohn and L. J. Sham, Phys. Rev. **140**, A1133 (1965).
[3] M. Foley, E. Smargiassi and P. A. Madden, J. Phys.: Condens. Matter **6**, 5231 (1994); J. A. Anta, B. J. Jesson, and P. A. Madden, Phys. Rev. B **58**, 6124 (1998); J. A. Anta and P. A. Madden, J. Phys.: Condens. Matter **11**, 6099 (1999); B. J. Jesson and P. A. Madden, J. Chem. Phys. **113**, 5924 (2000); **113**, 5935 (2000).
[4] D. J. González, L. E. González, J. M. López, and M. J. Stott, J. Chem. Phys. **115**, 2373 (2001).
[5] D. J. González, L. E. González, J. M. López, and M. J. Stott, Phys. Rev. B **65**, 184201 (2002).
[6] L. E. González, D. J. González, and J. M. López, J. Phys.: Condens. Matter **13**, 7801 (2001).
[7] D. J. González, L. E. González, J. M. López, and M. J. Stott, J. Non-Cryst. Solids **312-314**, 110 (2002).
[8] J. Blanco, D. J. González, L. E. González, J. M. López, and M. J. Stott, J. Non-Cryst. Solids **312-314**, 148 (2002); Phys. Rev. E

67, 041204 (2003).
[9] D. J. González, L. E. González, J. M. López, and M. J. Stott, Europhys. Lett. **62**, 48 (2003); Phys. Rev. E **69**, 031205 (2004).
[10] D. J. González, L. E. González, J. M. López, and M. J. Stott, J. Phys.: Condens. Matter **17**, 1429 (2005).
[11] B. J. Zhou, Y. A. Wang, and E. A. Carter, Phys. Rev. B **69**, 125109 (2004); B. J. Zhou, V. L. Ligneres, and E. A. Carter, J. Chem. Phys. **122**, 044103 (2005).
[12] A. Delisle, D. J. González, and M. J. Stott, Phys. Rev. B **73**, 064202 (2006).
[13] J. P. Gabathuler and S. Steeb, Z. Naturforsch. A **34a**, 1314 (1979); Y. Waseda and K. Suzuki, Z. Phys. B: Condens. Matter **20**, 339 (1975); Y. Waseda, K. Shinoda, K. Sugiyama, S. Takeda, K. Terashima, and J. M. Toguri, Jpn. J. Appl. Phys., Suppl. **34**, 4124 (1995); S. Takeda, *ibid.* **34**, 4889 (1995).
[14] Y. Waseda, *The Structure of Non-Crystalline Materials* (McGraw-Hill, New York, 1980).
[15] I. Stich, R. Car, and M. Parrinello, Phys. Rev. Lett. **63**, 2240 (1989); Phys. Rev. B **44**, 4262 (1991); I. Stich, Phys. Rev. A **44**, 1401 (1991); I. Stich, M. Parrinello, and J. M. Holender, Phys. Rev. Lett. **76**, 2077 (1996); V. Godlevsky, J. R. Chelikowsky, and N. Troullier, Phys. Rev. B **52**, 13281 (1995).
[16] N. Funamori and K. Tsuji, Phys. Rev. Lett. **88**, 255508 (2002).
[17] A. Delisle, D. J. González, and M. J. Stott, J. Phys.: Condens. Matter **18**, 3591 (2006).
[18] M.-C. Bellissent-Funel, R. Bellissent, and G. Tourand, J. Phys. F: Met. Phys. **11**, 139 (1981); M.-C. Bellissent-Funel, P. Chieux, D. Levesque, and J. J. Weis, Phys. Rev. A **39**, 6310 (1989).
[19] X. G. Gong, G. L. Chiarotti, M. Parrinello, and E. Tosatti, Phys. Rev. B **43**, 14277 (1991).
[20] M. Bernasconi, G. L. Chiarotti, and E. Tosatti, Phys. Rev. B **52**, 9988 (1995).
[21] J. E. Inglesfield, J. Phys. C **1**, 1337 (1968).
[22] L. F. Vereshchagin, S. S. Kabalkina, and Z. V. Toritskaya, Dokl. Akad. Nauk SSSR **158**, 1061 (1965); [Sov. Phys. Dokl. **9**, 894 (1965)]; C. E. Weir, G. J. Piermarini, and S. Block, J. Chem. Phys. **54**, 2768 (1971).
[23] L. Bosio, J. Chem. Phys. **68**, 1221 (1978).
[24] O. Degtyareva, M. I. McMahon, D. R. Allan, and R. J. Nelmes, Phys. Rev. Lett. **93**, 205502 (2004).
[25] X. G. Gong, G. L. Chiarotti, M. Parrinello and E. Tosatti, Europhys. Lett. **21**, 469 (1993).
[26] J. M. Holender, M. J. Gillan, M. C. Payne, and A. D. Simpson, Phys. Rev. B **52**, 967 (1995).
[27] J. M. Soler, E. Artacho, J. D. Gale, A. García, J. Junquera, P. Ordejón, and D. Sánchez-Portal, J. Phys.: Condens. Matter **14**, 2745 (2002).
[28] J. P. Perdew, K. Burke, and M. Ernzerhof, Phys. Rev. Lett. **77**, 3865 (1996).
[29] N. Troullier and J. L. Martins, Phys. Rev. B **43**, 1993 (1991).
[30] L. Kleinman and D. M. Bylander, Phys. Rev. Lett. **48**, 1425 (1982).
[31] R. L. McGreevy, A. Baranyai, and I. Ruff, Phys. Chem. Liq. **16**, 47 (1986).
[32] N. E. Cusak, *The Physics of Structurally Disordered Matter* (Adam-Hilger, Bristol, 1987).
[33] M. Inui, S. Takeda, and T. Uechi, J. Phys. Soc. Jpn. **61**, 3203 (1992).
[34] M. Boulahbak, J.-F. Wax, N. Jakse, and J. L. Bretonet, J. Phys.: Condens. Matter **9**, 4017 (1997); S. K. Lai, K. Horii, and M. Iwamatsu, Phys. Rev. E **58**, 2227 (1998).
[35] L. E. González, D. J. González, M. Silbert, and S. Baer, Mol. Phys. **99**, 875 (2001).
[36] M. W. C. Dharma-wardana and F. Perrot, Phys. Rev. Lett. **65**, 76 (1990); **65**, 2209(E) (1990).
[37] K. K. Mon, N. W. Ashcroft, and G. V. Chester, Phys. Rev. B **19**, 5103 (1979).